Surface Charge and Lanthanum Block of Calcium Current in Bullfrog Sympathetic Neurons

Brian M. Block,* William C. Stacey,# and Stephen W. Jones§
Departments of *Neurosciences, #Biomedical Engineering, and §Physiology and Biophysics, Case Western Reserve University, Cleveland, Ohio 44106 USA

ABSTRACT The density of surface charge associated with the calcium channel pore was estimated from the effect of extracellular ionic strength on block by La^{3+}. Currents carried by 2 mM Ba^{2+} were recorded from isolated frog sympathetic neurons by the whole-cell patch-clamp technique. In normal ionic strength (120 mM *N*-methyl-D-glucamine, NMG), La^{3+} blocked the current with high affinity (IC_{50} = 22 nM at 0 mV). La^{3+} block was relieved by strong depolarization in a time- and voltage-dependent manner. After unblocking, open channels reblocked rapidly at 0 mV, allowing estimation of association and dissociation rates for La^{3+}: $k_{on} = (7.2 \pm 0.7) \times 10^8$ M^{-1} s^{-1}, $k_{off} = 10.0 \pm 0.5$ s^{-1}. To assess surface charge effects, La^{3+} block was also measured in low ionic strength (12.5 mM NMG) and high ionic strength (250 mM NMG). La^{3+} block was higher affinity and faster by two- to threefold in 12.5 mM NMG, with little effect of 250 mM NMG. The data could be described by Gouy-Chapman theory with a surface charge density of ~1 e^-/3000–4000 $Å^2$. These results indicate that there is a small but detectable surface charge associated with the pore of voltage-dependent calcium channels.

INTRODUCTION

It is well known that ion channels can be affected by surface charges, located on membrane lipids or on the channel protein itself (Frankenhaeuser and Hodgkin, 1957; Green and Anderson, 1991; Hille, 1968; Hille, 1992). Surface charges exert their effects by creating a surface potential, which biases the voltage sensed by an ion channel. The surface potential can have large effects on channel gating, and may also affect ion permeation.

Previous studies of calcium currents in frog sympathetic neurons, using changes in $[Ba^{2+}]_o$, ionic strength, and pH to affect surface charge, concluded that the gating mechanism senses a rather large surface charge density (~1 e^-/100 $Å^2$), but the channel pore senses much less surface charge, <1 e^-/1500 $Å^2$ (Zhou and Jones, 1995, 1996). In fact, those studies were also consistent with the total absence of surface charge associated with permeation.

As a further test for effects of surface charge on permeation, we have examined the effect of extracellular ionic strength on the blockade of calcium channels by La^{3+}. If there is a surface charge associated with the channel pore, La^{3+} should be more potent in low ionic strength solutions. Because ions screen surface charge, the normal negative surface potential would be increased in low ionic strength. That surface potential would increase the local cation concentrations at the mouth of the pore. Because that effect depends on valence, it would be especially strong for a trivalent cation. The resulting increase in local $[La^{3+}]$ at low ionic strength would increase the effective blocking rate. We found that La^{3+} block is both faster and higher affinity in low ionic strength, and we have estimated the density of surface charge necessary to produce that effect.

Some results of this study have been reported as abstracts (Block and Jones, 1993; Block et al., 1998).

Received for publication 3 February 1997 and in final form 4 February 1998.

Address reprint requests to Dr. Stephen W. Jones Department of Physiology and Biophysics, Case Western Reserve University, Cleveland, OH 44106. Tel.: 216-368-5526; Fax: 216-368-3952; E-mail: swj@po.cwru.edu.

0006-3495/98/05/2278/07 $2.00

MATERIALS AND METHODS

Caudal paravertebral sympathetic neurons were isolated as previously described (Jones, 1987; Kuffler and Sejnowski, 1983). Isolated neurons were stored in supplemented L15 culture media at 4°C for up to 14 days. Whole-cell patch-clamp recordings (Hamill et al., 1981) were made from large spherical neurons (50.1 ± 1.5 pF, range 25–95 pF) at room temperature (22–24°C). Electrodes were pulled from 7052 or EN-1 glass (Garner Glass, Claremont, CA).

Approximately 90% of the Ca^{2+} current in these neurons is N-type (Jones and Marks, 1989). Ca^{2+} channel currents were isolated by replacing Na^+ and K^+ with the large impermeant cation *N*-methyl-D-glucamine (NMG), with 2 mM Ba^{2+} as the charge carrier. Extracellular solution compositions are shown in Table 1. The standard intracellular solution was 61.6 mM NMG · Cl, 2.5 mM NMG · HEPES, 10 mM NMG_2EGTA, 5 mM $Tris_2ATP$, 4 mM $MgCl_2$, 0.3 mM Li_2GTP, 14 mM phosphocreatine. Sucrose was added to maintain osmolarity where noted (Table 1). Chemicals were from Sigma Chemical Co. (St. Louis, MO), except for $LaCl_3$, which was Certified Grade from Fisher Scientific (Pittsburgh, PA). Solutions were applied by bath superfusion with gravity flow. We found that La^{3+} could bind to the polyethylene tubing and bath chamber and leach out into control solutions at low (nM) but detectable levels. To prevent this contamination, 10 or 100 μM EGTA was added to the control extracellular solutions, and the tubing was rinsed with EGTA before La^{3+} application. Currents in the absence of La^{3+} were not affected by the addition of up to 100 μM EGTA. For some data sets, the extent of block was inversely correlated with the time constant, even for data with the same nominal $[La^{3+}]$, which might indicate that our precautions did not completely prevent variation in $[La^{3+}]$ (see Eq. 2; Fig. 3 *C*). For measurements of inhibition by La^{3+}, the control value was the average of the current amplitudes before and after La^{3+} application.

Currents were recorded with an Axopatch 200 amplifier (Axon Instruments, Foster City, CA), Labmaster A-D interface (Axon Instruments), and an eight-pole Bessel low-pass filter (Frequency Devices, Haverhill, MA), and were stored on a personal computer. When recording only in control

TABLE 1 Extracellular solutions

	NMG · Cl	NMG · HEPES	Sucrose	$BaCl_2$	Specific viscosity	D/D_{CON}
12.5 NMG	10.0	2.5	215	2	1.39	0.80
120 NMG	117.5	2.5	0	2	1.11	1.00
120 NMG + sucrose	117.5	2.5	265*	2	1.31	0.85
250 NMG	250.0	2.5	0*	2	1.17	0.95

All concentrations are millimolar. Viscosity was calculated from the flow rate of the solution through a long narrow tube, and is presented as specific viscosity (relative to water). The measured specific viscosities were comparable to values interpolated from data for glucose (assumed to be similar to NMG) and sucrose (Weast, 1980). *D*, Diffusion coefficient, calculated from the reciprocal of the viscosity, expressed relative to the control solution (120 NMG). *For these experiments, 265 mM sucrose was added to the intracellular solution.

ionic strength (120 NMG), a Ag/AgCl pellet was used as the bath ground. When the ionic strength was varied during a given experiment or when recording with high or low ionic strength solutions, a 3 M KCl agar bridge was used as the bath ground to avoid junction potential changes at the ground electrode. Whole-cell series resistance was estimated from optimal correction of the capacity transient. Series resistance compensation was nominally ~90%. Currents were analog filtered at 2 kHz and digitally sampled at 5 kHz. A P/4 or P/5 protocol was used for linear leak and capacitance subtraction. pClamp (Axon Instruments) was used for data acquisition and initial analysis.

Analysis of the time course of La^{3+} reblocking required precautions to minimize contamination from activation and inactivation kinetics. Currents were recorded at 0 mV, where activation is rapid and nearly complete in 2 mM Ba^{2+} (Jones and Marks, 1989). Currents inactivated by 17.4 ± 0.8% during 320-ms depolarizations, which were used to measure La^{3+} reblocking in most experiments. Fits to the sum of two exponentials (i.e., one component for La^{3+} block and one for inactivation) gave inconsistent results, as the pulses used (generally 320 ms) were too brief to accurately define the time course of inactivation. (Measured from 2-s depolarizations, inactivation was described by $\tau_1 = 110$ ms, $\tau_2 = 1400$ ms, with 40% of the current noninactivating on that time scale; Werz et al. (1993).) Instead, the time constant for La^{3+} reblocking was measured by fitting to a single exponential from just after the time of peak current to where the current had nearly levelled off. In most cases, the duration fitted was at least three times the measured time constant.

Other fitting was done with the Solver utility of Excel (Microsoft, Redmond, WA), by minimizing the sum of the squared errors. Values reported in the text are mean ± SEM. Where noted, statistical significance was assessed using Student's *t*-test ($p < 0.05$).

RESULTS

Whole-cell currents carried by 2 mM Ba^{2+} through calcium channels in bullfrog sympathetic neurons were blocked by low concentrations of La^{3+} (Fig. 1). Measured at 0 mV, the IC_{50} for La^{3+} block was 22 nM in normal ionic strength. La^{3+} was even more potent in low ionic strength (12.5 NMG), with $IC_{50} = 9$ nM. Recovery from La^{3+} block was rapidly reversible in the presence of 10–100 μM EGTA (see Materials and Methods).

Channel unblocking by strong depolarization

La^{3+} block was voltage dependent, with partial relief of block upon strong depolarization (as briefly noted by Jones and Marks, 1989; see Thévenod and Jones, 1992, for data with Cd^{2+}). Unblocking was time and voltage dependent (Fig. 2). Brief conditioning pulses to +120 mV increased the current observed during a subsequent step to 0 mV (Fig. 2 *A*), reflecting the loss of La^{3+} block. In 30 nM La^{3+}, unblocking was faster at +120 mV than at +80 mV, τ = 0.90 ± 0.05 ms ($n = 4$) and 3.2 ± 0.3 ms ($n = 3$), respectively. Steps to +40 mV did not produce relief of block (Fig. 2 *B*).

Open channel block

We exploited the ability to transiently drive La^{3+} out of the channel to measure the association and dissociation rates (k_{on} and k_{off}) for La^{3+}, using the protocol illustrated in Fig. 3, *A* and *B*. After the step to +120 mV drove La^{3+} out of the channel, La^{3+} then reblocked the open channels during the

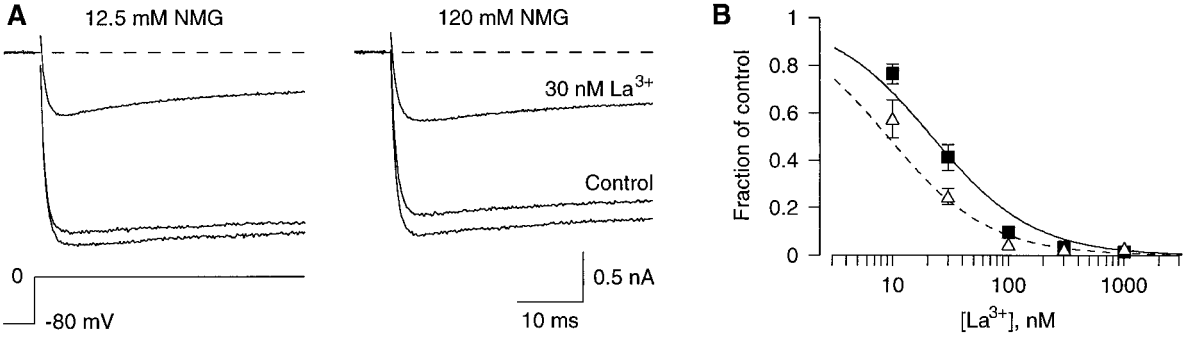

FIGURE 1 La^{3+} block of current through Ca^{2+} channels. (*A*) Reversible block by 30 nM La^{3+}, in low versus normal ionic strength (*left* and *right*, respectively). In each panel, the two larger inward currents (labeled Control) were recorded before La^{3+} and after recovery. In this and other figures, the dashed lines indicate zero current. Cell c5510. (*B*) The concentration dependence of La^{3+} block, in normal (■) and low (△) ionic strength. Currents were measured as the average during the last 2.5 ms of each step. The data were fitted to Langmuir isotherms with $IC_{50} = 22$ nM (normal) and $IC_{50} = 9$ nM (low ionic strength). Error bars are shown when larger than the symbols. Each point represents three to six cells, except $n = 2$ for 300 and 1000 nM La^{3+} in low ionic strength.

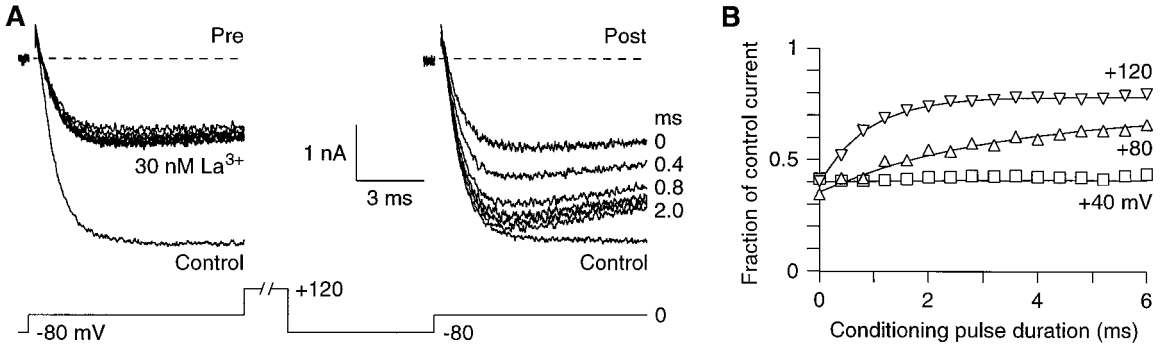

FIGURE 2 Partial relief of La^{3+} block by strong depolarization. (*A*) The protocol used to examine the time and voltage dependence of unblocking. Every 10 s, a brief prepulse was given to 0 mV (Pre), followed immediately by a variable conditioning pulse, here to +120 mV for 0–2 ms in 0.4-ms increments. After 6 ms at −80 mV, to allow the channels to close, a postpulse to 0 mV (Post) was given to assay the remaining La^{3+} block. For comparison, control currents are also shown—the average of currents recorded before La^{3+} and after recovery. For clarity, only the currents during the pre- and postpulse are shown. These currents were recorded in 120 NMG·Cl from cell d5713. (*B*) Dependence of unblocking on time and voltage. The current amplitude (relative to control) is plotted versus the duration of the depolarizing step to +40 mV (□), +80 mV (△), or +120 mV (▽). Currents were measured near the time of peak inward current (in La^{3+}) during each pre- and postpulse, from the protocol of *A*, for two to five cells at each voltage. The amount of unblocking is underestimated here, as some reblock occurs during the postpulse before the currents were measured, but that would not affect the observed time course of unblocking.

postpulse to 0 mV. At that voltage, channel activation is nearly at maximum (Jones and Marks, 1989), and inactivation is relatively slow (e.g., control records in Fig. 3, *A* and *B*), so the relaxation in the current during the postpulse reflects the kinetics of La^{3+} block of the open channel. We estimated k_{off} and k_{on} assuming bimolecular reaction kinetics, where the dissociation constant $K_D = k_{off}/k_{on}$, the fraction (f) of current remaining in La^{3+} is $f = K_D/([La^{3+}] + K_D)$, and the time constant of La^{3+} block (τ) is given by

$$1/\tau = [La^{3+}]k_{on} + k_{off}. \quad (1)$$

These relations can be combined to show that

$$\tau = f/k_{off}. \quad (2)$$

The usual method for estimating k_{off} and k_{on} would be to fit the data to Eq. 1, using a plot of $1/\tau$ versus $[La^{3+}]$. However, in that method, k_{off} is estimated from the y intercept, which is near zero (i.e., k_{off} is generally small relative to $1/\tau$). As a result, fits to Eq. 1 produced highly variable values for k_{off}, even when a weighted regression was used. In addition, the K_D calculated from k_{off}/k_{on} could be very different from the K_D estimated from the dose-response relationship for La^{3+} (Fig. 1 *B*).

Instead, we used Eq. 2 to calculate k_{off} directly from the experimentally observed τ and f, for each La^{3+} application. Fig. 3 *C* illustrates graphically that the averaged k_{off} values accurately reflect the relationship between τ and f. Next, k_{on} was calculated for each La^{3+} application from τ and k_{off}, using Eq. 1. The averaged values for k_{on} and k_{off} (Table 2) also describe well the relation between $1/\tau$ and $[La^{3+}]$ (Fig. 3 *D*). The linear relations in Fig. 3, *C* and *D*, are consistent with the assumption that La^{3+} block follows bimolecular kinetics.

We attempted to justify our method more rigorously, using simulated data sets. Each data set included five points at each of four concentrations (10, 30, 100, and 300 nM). The simulated measurements τ and f were calculated from k_{on} and k_{off} values (close to those for the 120 NMG data; Table 2), using Eqs. 1–2, and then random Gaussian noise was added (SD of noise = 25% of mean value). For 80 simulated data sets, the average fractional error (root mean squared error, divided by the known k_{on} or k_{off} value) was 0.12 for k_{on} and 0.10 for k_{off}. For comparison, the fitting procedure, minimizing the sum of squared errors for the relation between τ and $[La^{3+}]$, gave fractional errors of 0.18 for k_{on} and 0.29 for k_{off} for the same 80 data sets. Note that the fitting procedure gave especially poor estimates for k_{off}, as we had surmised from the actual experimental results. However, further simulations (8000 data sets) revealed that part of the error with our procedure was systematic, leading to overestimation of both k_{on} and k_{off} by 7–9% (for the range of values in Table 2). We do not consider that amount of error to be significant here, especially because the surface charge is estimated from the ratio of k_{on} values (see below). We prefer to use the analytic solution (Eqs. 1 and 2) to estimate k_{on} and k_{off}, because it uses both kinetic (τ) and steady-state (f) data, and it uses direct calculation rather than curve fitting.

La^{3+} block was faster in low ionic strength (Fig. 3 and Table 2). The primary effect was an increased k_{on}, but k_{off} was also slightly higher in low ionic strength (Fig. 3 *C*). Increased ionic strength (250 NMG) had little or no effect on k_{on}, but there was a small decrease in k_{off} (Table 2).

Estimation of the surface charge associated with permeation

Surface charges near the outer mouth of the channel pore would increase the local concentration of a cation (*C*) by a

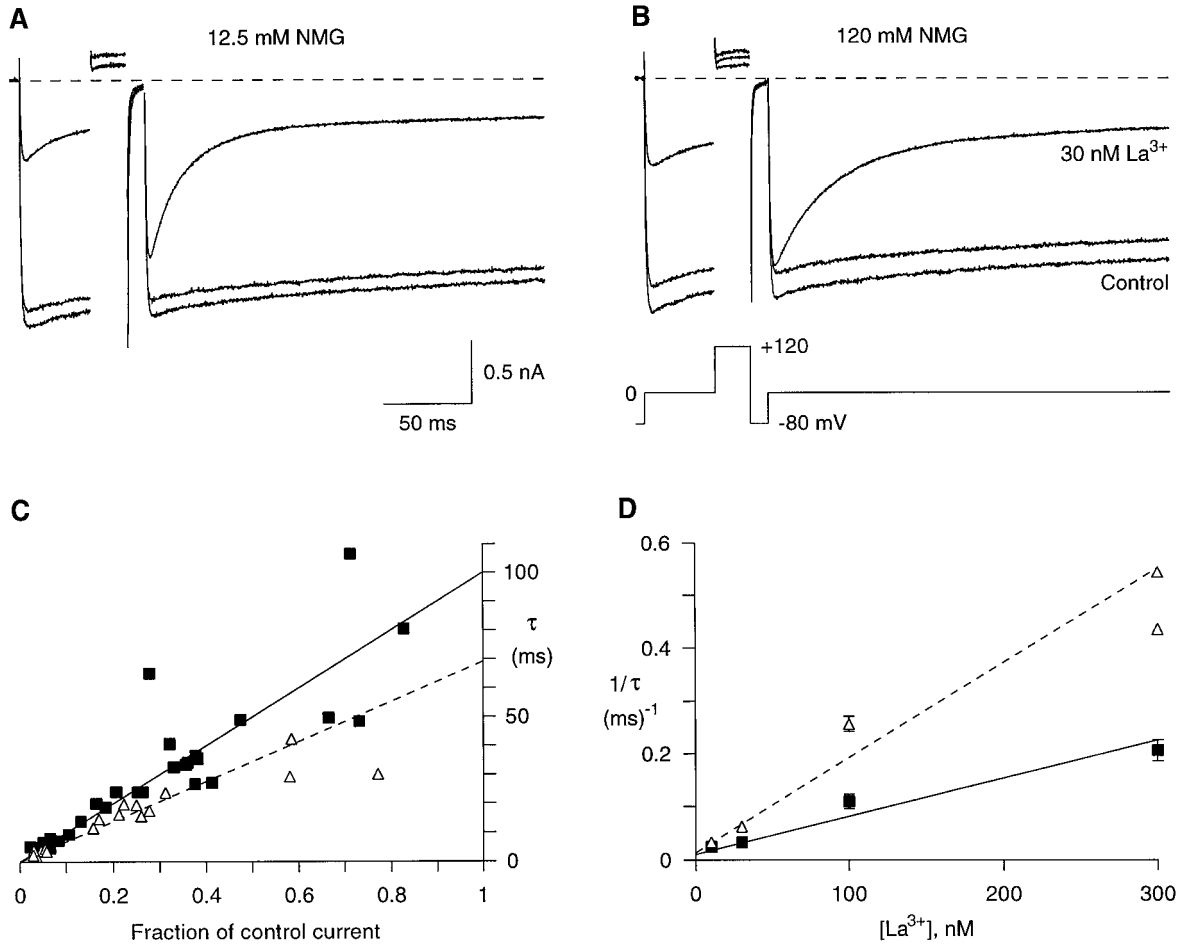

FIGURE 3 La^{3+} binding kinetics, measured from the time course of reblocking at 0 mV. Reblocking was compared in low (*A*) and normal (*B*) ionic strength. Currents are from the same cell as Fig. 1, with control currents recorded before and after La^{3+} application. The time-dependent relaxations during the postpulses in 30 nM La^{3+} reflect rebinding of La^{3+}, after the conditioning depolarization to +120 mV drove La^{3+} out of the channel. The scale bars in *A* also apply to *B*. (*C*) Estimation of the dissociation rate at 0 mV, in normal (■) and low (△) ionic strength. The time constant for reblocking (τ) was determined from a single exponential fit to the current during the postpulse (see Materials and Methods). Each data point is a different La^{3+} application ($n = 28$ in 16 cells, normal ionic strength; $n = 17$ in 7 cells, low ionic strength). The lines are drawn from Eq. 2, using the average k_{off} values (Table 2), in normal and low ionic strength (*solid* and *dashed lines*, respectively). (*D*) Concentration dependence of the time constant for reblocking by La^{3+}, in normal (■) and low (△) ionic strength. Values are means from 3–12 cells, with error bars (SEM) shown when larger than the size of the symbol, except that the individual data points are shown for 300 nM La^{3+} in low ionic strength, where $n = 2$. The lines are drawn assuming bimolecular kinetics (Eq. 1) for the mean k_{on} and k_{off} values (Table 2), not from linear fits to the data in this graph.

Boltzmann factor:

$$[C]_{Local} = [C]_{Bulk} \exp(-zF\psi/RT), \quad (3)$$

where ψ is surface potential, z is the charge on the ion, and F, R, and T have their usual thermodynamic meanings. That effect would be especially strong for a trivalent cation such as La^{3+}, and would be more evident at low ionic strength, where there is less screening of surface charge. Therefore, the increased k_{on} in low ionic strength could simply reflect an increased local $[La^{3+}]$. If so, the change in surface potential between solutions A and B can be estimated from

$$\Delta\psi = \psi_A - \psi_B = -(RT/zF)\ln(k_{on,A}/k_{on,B}), \quad (4)$$

As discussed further below, this assumes that the ratio of k_{on} values reflects the $[La^{3+}]$ ratio. The calculated $\Delta\psi$ values are given in Table 2.

The surface charge density (σ) is related to the surface potential and the solution composition by the Grahame equation (Grahame, 1947):

$$\sigma^2 G^2 = \sum[C_i]\{\exp(-z_i F\psi/RT) - 1\} \quad (5)$$

(G is a constant equal to 270 $Å^2 e^{-1} M^{1/2}$ at room temperature.) That equation is based on Gouy-Chapman theory, which assumes that ions screen surface charge without direct binding.

Because the experimental measurement is not ψ but $\Delta\psi$, σ cannot be calculated directly. For a wide range of assumed σ values, we solved Eq. 5 for ψ in each ionic strength, using a numerical bisection method (Zhou and Jones, 1995). Each calculation yielded estimates of $\Delta\psi$, for normal versus low and normal versus high ionic strength.

TABLE 2 Kinetics of La^{3+} block

		IC_{50} (nM)	k_{on} (nM^{-1} s^{-1})	k_{off} (s^{-1})	k_{off}/k_{on} (nM)	$\Delta\Psi$ (mV)	$1/\sigma$ ($Å^2/e^-$)
	12.5 NMG	9.1	1.79 ± 0.15 (n = 17)*	14.4 ± 1.0 (n = 17)#	8.1		4020
	120 NMG	22	0.72 ± 0.07 (n = 24)*	10.0 ± 0.5 (n = 28)#	14	−7.8	
	120 NMG + sucrose		0.49 ± 0.05 (n = 22)	9.4 ± 0.6 (n = 28)§	19		
	250 NMG		0.54 ± 0.06 (n = 19)	6.7 ± 0.5 (n = 24)§	12	−0.8	
Corrected for viscosity	12.5 NMG		2.24 ± 0.19 (n = 17)	18.1 ± 1.3 (n = 17)	8.1		3050
	120 NMG		0.72 ± 0.07 (n = 24)	10.0 ± 0.5 (n = 28)	14	−9.7	
	120 NMG + sucrose		0.57 ± 0.06 (n = 22)	11.0 ± 0.8 (n = 28)	19		
	250 NMG		0.56 ± 0.06 (n = 19)	7.0 ± 0.5 (n = 24)	12	0.1	

Symbols (*, #, §) mark pairs of rate constants that were significantly different from each other. IC_{50} values are from Fig. 1 *B*. k_{on} and k_{off} were calculated from Eqs. 1 and 2 as described in the text. In some initial experiments, the La^{3+} concentration was not well controlled, because of its leaching out of the tubing. Because k_{off} was independent of $[La^{3+}]$, such experiments could be used to calculate k_{off} (Eq. 2), so the sample size was larger for k_{off} than k_{on}. $\Delta\Psi$ was calculated from Eq. 4 for each pair of k_{on} values, and σ values were estimated as described in the text. In the lower half of the table, k_{on} and k_{off} were corrected for viscosity by dividing by the D/D_{CON} ratios (Table 1), and $\Delta\Psi$ and σ were then calculated from those corrected values.

The best value for σ (Table 2) was determined by minimizing the sum of the squared errors for the two comparisons.

When ionic strength is varied, $\Delta\psi$ depends on σ in a biphasic manner, so a small $\Delta\psi$ might reflect either a very low σ or a very high σ (Becchetti et al., 1992; Zhou and Jones, 1995). For the best solution with low σ (1 e^-/4020 $Å^2$, Table 2), the calculated $\Delta\psi$ was −7.3 mV for the normal versus low ionic strength comparison, and +1.4 mV for normal versus high ionic strength, comparable to the observed values (Table 2). In contrast, the best fit with high σ (1 e^-/27 $Å^2$) gave $\Delta\psi$ values of similar magnitude for the two comparisons (−3.1 mV and +3.6 mV, respectively), so the sum of squared errors in the fit was eightfold lower for the low σ solution.

Because large changes in [NMG] were required to vary ionic strength, sucrose was added to certain solutions to maintain equal intra- and extracellular osmolality (Table 1). The changes in [NMG] and [sucrose] affected the solution viscosity and thus diffusion coefficients. If La^{3+} block is a diffusion-limited reaction, as suggested by the extremely high k_{on}, both k_{on} and k_{off} would be affected by viscosity (Miller, 1990; Schurr, 1970). After correction for viscosity, the estimated surface charge density was higher (σ = 1 e^-/3050 $Å^2$; Table 2), but still ~30-fold less than the surface charge associated with gating (Zhou and Jones, 1995, 1996).

DISCUSSION

La^{3+} block was voltage dependent, as block could be relieved by strong depolarizations in a time- and voltage-dependent manner. The voltage dependence is evidence that La^{3+} acts by binding to a site in the channel pore (e.g., Lansman et al., 1986; Lansman, 1990; Kuo and Hess, 1993).

Surface charge and permeation

Low ionic strength increased both the potency and the rate of La^{3+} block, which is strong qualitative evidence that the channel pore does sense a surface charge. The estimate of 1 e^-/3000–4000 $Å^2$ is consistent with the upper limit from previous work (Zhou and Jones, 1995, 1996). It predicts a small surface potential, ψ = −4 to −6 mV in normal ionic strength, and thus a relatively small (1.4–1.6-fold) increase in the concentration of a divalent cation near the pore. As Kuo and Hess (1992) concluded, this effect would not play a major role in the selectivity of calcium channels for divalent over monovalent cations. The conclusion that surface charge has less effect on permeation than on gating is consistent with several previous studies on calcium channels (Wilson et al., 1983; Coronado and Affolter, 1986; Kuo and Hess, 1992; Zhou and Jones, 1995; but see Smith et al., 1993). In particular, Kuo and Hess (1992) used an approach similar to ours (the effect of ionic strength on block by Ca^{2+} of current carried by Li^+) to estimate a charge density of 1 e^-/600 $Å^2$ for L-channels of PC12 cells.

Our quantitative estimate of surface charge density required several assumptions. As noted above, if binding of La^{3+} is assumed to be diffusion limited, the estimated surface charge density is slightly larger (1 e^-/3050 $Å^2$, versus 1 e^-/4020 $Å^2$ without "correction" for solution viscosity). Furthermore, the calculation is based on Gouy-Chapman theory, which considers the surface potential at zero distance from the surface charge. We used Gouy-Chapman theory because of its relative simplicity (one free parameter, σ), and because of the lack of information on the actual geometry of the channel pore. An alternative interpretation is that the same surface charge is associated with both gating and permeation, but the entrance to the channel pore is at a much greater electrical distance from the surface charge, as Coronado and Affolter (1986) concluded for skeletal muscle L-type calcium channels. In that case, it would still be true that the surface potential would be much larger at the voltage sensor than at the pore. The surface charge could be either on plasma membrane lipids, or on the channel protein itself.

In addition, the change in surface potential was calculated by assuming that the observed two- to threefold increase in

k_{on} for La^{3+} at low ionic strength implied a two- to threefold increase in local $[La^{3+}]$ (Eq. 4). That interpretation could be affected by competition between La^{3+} and Ba^{2+}, because local $[Ba^{2+}]$ would also increase. Increased occupancy of the pore by Ba^{2+} might interfere with La^{3+} entry, decreasing the observed k_{on}. If there were a single binding site within the pore, this effect would be small, because the bulk $[Ba^{2+}]$ was only 2 mM, whereas the current was half-saturated at bulk $[Ba^{2+}] = 23.5$ mM in normal ionic strength (Zhou and Jones, 1995). From Eq. 3 with $\Delta\psi = -9.7$ mV, local $[Ba^{2+}]$ would increase twofold at low ionic strength, and pore occupancy would increase from 8% to 15%, which would have a negligible effect on La^{3+} entry. But the situation could be more complicated for a multiion pore. With the standard two-site models for calcium channel permeation, one site would essentially always be occupied at mM concentrations of Ba^{2+}, with the observed saturation of current at high $[Ba^{2+}]$ reflecting occupancy of the second site (Hess and Tsien, 1984; Almers and McCleskey, 1984). The rate of block by La^{3+} would primarily reflect entry of La^{3+} into pores already occupied by a single Ba^{2+} ion. As long as Ba^{2+} remains well below the concentration producing half-maximum current, occupancy by Ba^{2+} (and thus the k_{on} for La^{3+}) would change little, even for a two-ion pore. This is supported by the data of Kuo and Hess (1993) for L-type calcium channels, where the k_{on} for Cd^{2+} decreased with increasing Ba^{2+}, with the same apparent K_D as the conductance of the channel for Ba^{2+}. Thus Ba^{2+}–La^{3+} competition should not affect the k_{on} for La^{3+} with the relatively low $[Ba^{2+}]$ used here, so the increased k_{on} at low ionic strength is likely to be a direct reflection of an increase in local $[La^{3+}]$.

However, a small increase in occupancy of the pore by Ba^{2+} (e.g., 8–15%) could significantly affect the k_{off} for La^{3+} in a two-ion pore. Dissociation of La^{3+} occurs primarily from the doubly occupied state of the pore, because occupancy of the second site by Ba^{2+} destabilizes La^{3+} binding. Thus the increased k_{off} in low ionic strength (Table 2) could result from an increased local $[Ba^{2+}]$.

It has been suggested that NMG might block calcium channels (Kuo and Hess, 1992). If so, the increased potency of La^{3+} in low [NMG] might reflect relief of NMG block, not reduction of ionic strength. That does not seem likely, as most of the effect on La^{3+} block occurred between 10 mM and 117.5 mM NMG, whereas the effect of NMG on conductance for Ba^{2+} (assuming that it resulted from NMG block, not screening of surface charge) had an apparent K_D of 320 mM (Zhou and Jones, 1995). That is, a change in NMG occupancy large enough to produce a threefold change in k_{on} for La^{3+} between 10 mM and 117.5 mM NMG would produce strong channel block on its own, which was not observed (Zhou and Jones, 1995). We conclude that the effect of [NMG] on La^{3+} block, and the effect of [NMG] on channel conductance (Zhou and Jones, 1995), reflect screening of a small amount of surface charge.

La^{3+} block of calcium channels

Qualitatively, La^{3+} block resembled Cd^{2+} block (Thévenod and Jones, 1992), but La^{3+} had a much higher affinity, $K_D = 14$ nM versus 400 nM for Cd^{2+} (calculated as k_{off}/k_{on}). The lower affinity for Cd^{2+} reflected both a sixfold lower k_{on} (1.2×10^8 M^{-1} s^{-1}) and a fivefold higher k_{off} (50 s^{-1}) for Cd^{2+}. Some of the difference in k_{on} can be attributed to surface charge: for 1 e^-/3050 Å^2, $\psi = -6.5$ mV in normal ionic strength, which would increase the local $[Cd^{2+}]$ by 1.7-fold and $[La^{3+}]$ by 2.1-fold, giving intrinsic $k_{on(\psi = 0)}$ values of 3.4×10^8 M^{-1} s^{-1} for La^{3+}, and 0.72×10^8 M^{-1} s^{-1} for Cd^{2+}.

The apparent K_D for La^{3+} found here (22 nM from steady-state block; 14 nM from k_{off}/k_{on}) is lower than that in previous reports for La^{3+} block of Ca^{2+} channels, partly because of our use of relatively low $[Ba^{2+}]$. (As discussed above, the increased pore occupancy in high $[Ba^{2+}]$ would increase k_{off}, and near saturation k_{on} would also decrease.) Representative apparent K_D values for La^{3+} block of vertebrate high voltage-activated calcium channels are 163 nM (in 5 mM Ba^{2+}, cultured dorsal horn neurons; Reichling and MacDermott, 1991), 750 nM (in 2.5 mM Ca^{2+} and 5 mM Mg^{2+}, cardiac cells; Nathan et al., 1988), 900 nM (in 50 mM Ba^{2+}, neuroblastoma cells; Narahashi et al., 1987), and 14 μM (in 110 mM Ba^{2+}, skeletal muscle L channels; Lansman, 1990). Lansman (1990) also found $k_{on} = 0.14 \times 10^8$ M^{-1} s^{-1} and $k_{off} = 208$ s^{-1} at 0 mV; much of the difference from our values can be attributed to the 55-fold higher Ba^{2+} in that study. However, it is clear that calcium channels do differ in their sensitivity to di- and trivalent cations (Narahashi et al., 1987; Mlinar and Enyeart, 1993), and these differences may provide important clues to mechanisms of ion selectivity and permeation.

We thank Drs. R. V. Edwards, D. L. Feke, and C. A. Obejero-Paz for helpful discussions.

Supported in part by National Institutes of Health grant NS 24471 to SWJ, who was an Established Investigator of the American Heart Association. BMB and WCS are also supported by fellowships from the National Institutes of Health Medical Scientist Training Program.

REFERENCES

Almers, W., and E. W. McCleskey. 1984. Nonselective conductance in calcium channels of frog muscle: calcium selectivity in a single-file pore. *J. Physiol. (Lond.).* 353:585–608.

Becchetti, A., A. Arcangeli, M. R. Del Bene, M. Olivotto, and E. Wanke. 1992. Intra and extracellular surface charges near Ca^{2+} channels in neurons and neuroblastoma cells. *Biophys. J.* 63:954–965.

Block, B. M., and S. W. Jones. 1993. Lanthanum block of N-type calcium current in bullfrog sympathetic neurons. *Biophys. J.* 64:A319 (Abstr.).

Block, B. M., W. C. Stacey, and S. W. Jones. 1998. Effect of ionic strength on lanthanum block of calcium current in bullfrog sympathetic neurons. *Biophys. J.* 74:A245 (Abstr.).

Coronado, R., and H. Affolter. 1986. Insulation of the conduction pathway of muscle transverse tubule calcium channels from the surface charge of bilayer phospholipid. *J. Gen. Physiol.* 87:933–953.

Frankenhaeuser, B., and A. L. Hodgkin. 1957. The action of calcium on the electrical properties of squid axons. *J. Physiol. (Lond.).* 137:218–244.

Grahame, D. C. 1947. The electrical double layer and the theory of electrocapillarity. *Chem. Rev.* 41:441–501.

Green, W. N., and O. S. Andersen. 1991. Surface charges and ion channel function. *Annu. Rev. Physiol.* 53:341–359.

Hamill, O. P., A. Marty, E. Neher, B. Sakmann, and F. J. Sigworth. 1981. Improved patch-clamp techniques for high resolution current recording from cells and cell-free membrane patches. *Pflügers Arch.* 391:85–100.

Hess, P., and R. W. Tsien. 1984. Mechanism of ion permeation through calcium channels. *Nature.* 309:453–456.

Hille, B. 1968. Charges and potentials at the nerve surface. Divalent ions and pH. *J. Gen. Physiol.* 51:221–236.

Hille, B. 1992. Ionic Channels of Excitable Membranes, 2nd Ed. Sinauer Associates, Sunderland, MA.

Jones, S. W. 1987. Sodium currents in dissociated bull-frog sympathetic neurones. *J. Physiol. (Lond.).* 389:605–627.

Jones, S. W., and T. N. Marks. 1989. Calcium currents in bullfrog sympathetic neurons. I. activation kinetics and pharmacology. *J. Gen. Physiol.* 94:151–167.

Kuffler, S. W., and T. J. Sejnowski. 1983. Peptidergic and muscarinic excitation at amphibian sympathetic synapses. *J. Physiol. (Lond.).* 341: 257–278.

Kuo, C.-C., and P. Hess. 1992. A functional view of the entrances of L-type calcium channels: estimates of the size and surface potential at the pore mouths. *Neuron.* 9:515–526.

Kuo, C.-C., and P. Hess. 1993. Characterization of the high-affinity Ca^{2+} binding sites in the L-type Ca^{2+} channel pore in rat phaeochromocytoma cells. *J. Physiol. (Lond.).* 466:657–682.

Lansman, J. B. 1990. Blockade of current through single calcium channels by trivalent lanthanide cations: effect of ionic radius on the rates of ion entry and exit. *J. Gen. Physiol.* 95:679–696.

Lansman, J. B., P. Hess, and R. W. Tsien. 1986. Blockade of current through single calcium channels by Cd^{2+}, Mg^{2+}, and Ca^{2+}. Voltage and concentration dependence of calcium entry into the pore. *J. Gen. Physiol.* 88:321–347.

Miller, C. 1990. Diffusion controlled binding of a peptide neurotoxin to its K^+ channel receptor. *Biochemistry.* 29:5320–5325.

Mlinar, B., and J. J. Enyeart. 1993. Block of current through T-type calcium channels by trivalent metal cations and nickel in neural rat and human cells. *J. Physiol. (Lond.).* 469:639–652.

Narahashi, T., A. Tsunoo, and M. Yoshii. 1987. Characterization of two types of calcium channels in mouse neuroblastoma cells. *J. Physiol. (Lond.).* 383:231–249.

Nathan, R. D., K. Kanai, R. B. Clark, and W. Giles. 1988. Selective block of calcium current by lanthanum in single bullfrog atrial cells. *J. Gen. Physiol.* 91:549–572.

Reichling, D. B., and A. B. MacDermott. 1991. Lanthanum actions on excitatory amino acid-gated currents and voltage-gated calcium currents in rat dorsal horn neurons. *J. Physiol. (Lond.).* 441:199–218.

Schurr, J. M. 1970. The role of diffusion in bimolecular solution kinetics. *Biophys. J.* 10:700–716.

Smith, P. A., F. M. Ashcroft, and C. M. S. Fewtrell. 1993. Permeation and gating properties of the L-type calcium channel in mouse pancreatic β cells. *J. Gen. Physiol.* 101:767–797.

Thévenod, F., and S. W. Jones. 1992. Cadmium block of calcium current in frog sympathetic neurons. *Biophys. J.* 63:162–168.

Weast, R. C., editor. 1980. CRC Handbook of Chemistry and Physics, 60th Ed. CRC Press, Boca Raton, FL. D-239, D-270.

Werz, M. A., K. S. Elmslie, and S. W. Jones. 1993. Phosphorylation enhances inactivation of N-type calcium channel current in bullfrog sympathetic neurons. *Pflügers Arch.* 424:538–545.

Wilson, D. L., K. Morimoto, Y. Tsuda, and A. M. Brown. 1983. Interaction between calcium ions and surface charge as it relates to calcium current. *J. Membr. Biol.* 72:117–130.

Zhou, W., and S. W. Jones. 1995. Surface charge and calcium channel saturation in bullfrog sympathetic neurons. *J. Gen. Physiol.* 105: 441–462.

Zhou, W., and S. W. Jones. 1996. The effects of external pH on calcium channel currents in bullfrog sympathetic neurons. *Biophys. J.* 70: 1326–1334.